Acta Pharmaceutica Sinica B 2018;8(3):478–487

Chinese Pharmaceutical Association
Institute of Materia Medica, Chinese Academy of Medical Sciences

Acta Pharmaceutica Sinica B

www.elsevier.com/locate/apsb
www.sciencedirect.com

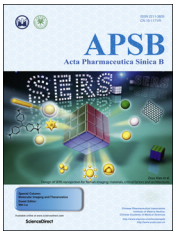

ORIGINAL ARTICLE

Activation of an unconventional meroterpenoid gene cluster in *Neosartorya glabra* leads to the production of new berkeleyacetals

Tao Zhang[a,†], Jun Wan[a,†], Zhajun Zhan[b], Jian Bai[a], Bingyu Liu[a], Youcai Hu[a,*]

[a]*State Key Laboratory of Bioactive Substance and Function of Natural Medicines, Institute of Materia Medica, Chinese Academy of Medical Sciences & Peking Union Medical College, Beijing 100050, China*
[b]*College of Pharmaceutical Science, Zhejiang University of Technology, Hangzhou 310014, China*

Received 9 September 2017; received in revised form 28 October 2017; accepted 11 November 2017

KEY WORDS

Neosartorya glabra;
Meroterpenoid;
Berkeleyacetals;
Genome mining;
Cryptic gene cluster;
Biosynthesis

Abstract Fungal genomes carry many gene clusters seemingly capable of natural products biosynthesis, yet most clusters remain cryptic or down-regulated. Genome mining revealed an unconventional paraherquonin-like meroterpenoid biosynthetic gene cluster in the chromosome of *Neosartorya glabra*. The cryptic or down-regulated pathway was activated by constitutive expression of pathway-specific regulator gene *berA* encoded within *ber* biosynthetic gene cluster. Chemical analysis of mutant *Ng*-OE: *berA* extracts enabled the isolation of four berkeleyacetal congeners, in which two of them are new. On the basis of careful bioinformatic analysis of the coding enzymes in the *ber* gene cluster, the biosynthetic pathway of berkeleyacetals was proposed. These results indicate that this approach would be valuable for discovery of novel natural products and will accelerate the exploitation of prodigious natural products in filamentous fungi.

*Corresponding author.
E-mail address: huyoucai@imm.ac.cn (Youcai Hu).
†These authors made equal contribution to this work.
Peer review under responsibility of Institute of Materia Medica, Chinese Academy of Medical Sciences and Chinese Pharmaceutical Association.

https://doi.org/10.1016/j.apsb.2017.12.005

1. Introduction

Meroterpenoids constitute an important family of hybrid natural products partially derived from terpenoid pathways, which have remarkably commercial and research values due to their diverse arrays of bioactivities and complex molecular architectures[1,2]. 3,5-Dimethylorsellinic acid (DMOA), an aromatic tetraketide intermediate widely synthesized by fungi, especially in the family Trichocomaceae, is further transformed into varied fascinating meroterpenoids.

Berkeleyacetals are heavily oxidized DMOA-derived meroterpenoids identified from *Penicillium rubrum* Stoll[3], and possess a unique and congested pentacyclic ring skeleton. Analogues, including miniolutelides, berkeleydione, berkeleytrione, dhilirolides, and paraherquonin have been isolated from several fungi in the genus *Penicillium*[4–9]. Interestingly, berkeleyacetals, berkeleydione and berkeleytrione reportedly inhibited matrix metalloproteinase-3 and caspase-1 effectively, in which berkeleyacetal C and berkeleydione were tested in antitumor screen for human cell line assay in NCI Developmental Therapeutics Program[3,5]. Considering their biological properties, biosynthetic studies or engineering of natural products with the berkeleyacetal scaffold could definitely contribute toward clarifying the bioprocesses and facilitate the development of promising anticancer pharmaceuticals.

Genome mining of sequenced fungi has yielded new natural products with interesting bioactivities and structures, and a group of down-regulated or cryptic biosynthetic gene clusters were characterized and elucidated[10–13]. Previous studies have demonstrated that genome mining, particularly the induction of down-regulated or cryptic secondary metabolic pathways by overexpressing of cluster-specific transcriptional activator genes, is a promising and more targeted-strategy[10,11,14–17].

Neosartorya glabra was reported to produce numbers of natural products, such as glabramycins A–C[18], sartoryglabrins A–C[19], neosarphenols A and B, methoxyvermistatin, vermistatin, penicillide, purpactin, phialophoriol, etc.[20]. Whole genome sequencing of *N. glabra* revealed that its genome contains 17 polyketide synthetases (PKSs) gene clusters, 4 nonribosomal peptide synthetases (NRPSs) gene clusters, 3 PKS-NRPS hybrid gene clusters, and 5 terpene gene clusters, which far exceeds the total number of known natural products isolated from *N. glabra*[17–21]. Interestingly, we mined the genome of *N. glabra* and identified a paraherquonin-like meroterpenoid biosynthetic gene cluster *ber* that contains 5 additional genes other than *prh* cluster in *P. brasilianum* NBRC 6234 for paraherquonin biosynthesis[8]. Therefore, the unconventional gene cluster suggests it might be responsible for production of novel meroterpenoids. In this study, we demonstrated that overexpression of a pathway-specific regulator gene *berA* encoded within a down-regulated or cryptic, meroterpenoid biosynthetic gene cluster in *N. glabra* could stimulate the activation in a relatively straightforward fashion and 4 berkeleyacetal congeners or derivatives were characterized. This work provides the strategy to activate cryptic gene clusters by overexpressing pathway-specific regulator gene and help broaden our knowledge of the mechanism and pathway engineering of berkeleyacetals.

2. Materials and methods

2.1. Strains and cultivation conditions

The *N. glabra* strain was obtained from China General Microbiological Culture Collection Center and was used as the parental strain in our study. Both the wild-type and its mutant strains were grown on MEPA (3% malt extract broth, BD; 0.3% soy flour, 1.5% agar) for both secondary metabolites production and mRNA extraction at 28 °C. For gene overexpression in *N. glabra*, potato dextrose agar (BD) with 1.2 mol/L sorbitol and 400 μg/mL G418 was used for protoplast regeneration and antibiotic resistance selection. *Escherichia coli* Trans1-T1 was used for routine plasmid cloning. *Saccharomyces cerevisiae* strain BJ5464-NpgA (*MATα ura3-52 his3-Δ200 leu2-Δ1 trp1pep4:HIS3 prb1Δ1.6R can1 GAL*) was used for *in vivo* yeast DNA recombination cloning and the yeast expression host[22]. YPD (2% peptone, 1% yeast extract, 2% dextrose) was used for the routine growth of yeast strain BJ5464-NpgA and its derivatives at 30 °C. SD dropout medium was used for selection of plasmids transformed into *S. cerevisiae*. For protein expression under *ADH2* promoter (*ADH 2p*) in *S. cerevisiae*, the yeast transformant was initially grown in the appropriate SD dropout liquid medium and then was transferred to the liquid YPD medium for further culture for 5 days. LB medium was used for culturing *E. coli*.

2.2. Sequencing and bioinformatic analysis

The genomic DNA of *N. glabra* used for sequencing was prepared from mycelium grown in stationary liquid culture (3% malt extract broth, BD; 0.3% soy flour). The shotgun sequencing was performed at Beijing Genomics Institute (Shenzhen, China) with the Illumina Hiseq. 2000 sysem. The contigs that assembled and annotated by SOAP denovo 1.05 were formatted to BLAST database for basic local BLAST search[23]. AntiSMASH platform was used for genome mining and bioinformatic analysis of secondary metabolites biosynthetic clusters[24]. Gene predictions were performed using the FGENESH program (Softberry) and manually checked by comparing with homologous proteins in the GenBank database. Functional domains in the translated protein sequences were predicted using Conserved Domain Search (NCBI) or InterproScan (EBI).

2.3. N. glabra RNA preparation, cDNA preparation, and reverse transcription-PCR (RT-PCR)

Mycelia of *N. glabra* and mutant *Ng*-OE: *berA* were inoculated into MEPA medium, incubated at 28 °C for 5 days, and collected for lyophilization. The total RNAs from culture of the wild type strain and mutant were extracted using the protocols as described previously[25]. The genomic DNA was further removed by RNase-free DNase I (Takara). RNA was purified by RNAclean purification kit (Tiangen). RNA integrity was confirmed by electrophoresis on TAE buffer (Tris-acetate-EDTA) agarose gel. The first-strand cDNA was synthesized from 500 ng of total RNA by EasyScript® reverse transcriptase (Transgen) with random primers and oligo-dT_{18} primer (Takara) as described by the manufacturer. The gene expression level was analyzed by PCR using the specific primers listed in Supplementary information Table S1 and cDNA template. For BerA expression, PCR was performed with Q5 high-fidelity DNA polymerase (New England Biolabs) in the presence of 50 ng of reverse transcribed RNA. Primers are listed in Supplementary information Table S1.

2.4. Plasmid construction

Primers are listed in Supplementary information Table S1. Yeast expression plasmid pYET containing TRP1 auxotrophic marker

was used for construction of the heterologous expression plasmid by *in vivo* homologous recombination in yeast. For polyketide synthase BerP expression, primers pairs BerP-S1 for/rev, BerP-S2 for/rev, and BerP-S3 for/rev were used to amplify three DNA fragments of *berP* cDNA and were transformed into *S. cerevisiae* BJ5464-NpgA simultaneously with *Nde* I/*Pme* I digested pYET to create the plasmid pZT1. Yeast competent cell preparation and transformation were performed with a Frozen-EZ Yeast Transformation II kit (Zymo Research) according to the manufacture's protocol. Yeast plasmids were prepared by a Yeast Plasmid Miniprep kit (Solarbio) and transformed into *E. coli* strain Trans1-T1 for propagation and sequencing.

For construction of overexpression cassettes of *berA*, the gene *berA* was amplified from *N. glabra* genomic DNA using primers listed in Supplementary information Table S1. The constitutive *gPdA* promoter from *Aspergillus nidulans* (glyceraldehydes-3-phosphate dehydrogenase promoter) and G418 resistance gene fragment were amplified in which plasmids pRF-HUE and pYWL42 act as DNA templates. The three DNA fragments (*gPdA*, G418, and *berA* DNA fragments) were ligated into the linearized vector pET30a, which was digested with *Hin*d III and *Eco*R I. The plasmids in the correct transformant screened by colony PCR were sequenced and used as template to amplify the overexpression cassette. Before transformation, the PCR products of overexpression cassette was recovered by a gel extraction kit (Omega, Cat. No. D2500-02) according to the manufacturer's protocol and dissolved in STC buffer (1.2 mol/L sorbitol, 10 mmol/L $CaCl_2$, 10 mmol/L Tris HCl, pH 7.5).

2.5. Fungal transformation and gene overexpression in *N. glabra*

Polyethylene glycol-mediated transformation of *N. glabra* was performed essentially as described previously for *A. nidulans*[26,27] except that the protoplasts were prepared with 3 mg/mL lysing enzymes (Sigma–Aldrich) and 2 mg/mL yatalase (Takara). Briefly, fresh spores of *N. glabra* were collected and then induced to young germling with concentration of 10^8 spores mL^{-1} for 24 h at 28 °C with 150 rpm agitation. Young mycelia were harvested, washed twice with osmotic medium (1.2 mol/L $MgCl_2$, 10 mmol/L sodium phosphate [pH 5.8]), and resuspended in the enzyme cocktail solution at 30 °C overnight. After washing twice with STC buffer (1.2 mol/L sorbitol, 10 mmol/L $CaCl_2$, 10 mmol/L Tris–HCl, [pH 7.5]), protoplasts were gently mixed with DNA and incubated for 50 min on ice. One milliliter of PEG 4000 solution (60% PEG 4000, 50 mmol/L $CaC1_2$, 50 mmol/L Tris-HCI [pH 7.5]) was added to 100 μL of protoplast mixture, and the mixture was incubated for 20 min at ambient temperature and spread on the regeneration selection medium (PDA, 1.2 mol/L sorbitol, 400 μg/mL G418). After incubation at 28 °C for 4–5 days, the transformants were inoculated on fresh PDB selection medium with stationary incubation for about 4 days to confirm the genotype by diagnostic PCRs after preparation of the genomic DNA. The specific primers used are shown in Supplementary information Table S1.

2.6. Chemical reagents and chemical analyses

All solvents and chemicals used this study are of analytical grade (for extraction) or LC–MS grade (for LC–MS analysis). Cultures of *N. glabra*, or *S. cerevisiae* cells were extracted with ethyl acetate. After 12,000 rpm, 10 min centrifugation (Eppendorf AG, MiniSpin, Hamburg, Germany), the supernatant organic phase was dried (Labconco Corporation, Dry Evaporators, Concentrators & Cold Traps, MO, USA) and solubilized in acetonitrile for LC–MS analyses. All LC–MS analyses were performed on a Waters ACQUITY H-Class UPLC–MS with a PDA detector and a QDA mass detector (ACQUITY UPLC® BEH, 1.7 μm, 50 mm × 2.1 mm, C18 column) using positive and negative mode electrospray ionization with a linear gradient of 5%–99% ACN–H_2O (*v*/*v*, 0.02% formic acid) for 8 min followed by 99% ACN–H_2O (*v*/*v*, 0.02% formic acid) for 4 min with a flow rate of 0.4 mL/min. X-ray data were collected using a Rigaku MicroMax 002+ instrument. The optical rotations were measured on a Jasco P2000 polarimeter, UV spectra were detected by a Jasco V650 spectrophotometer (JASCO, Corporation, Tokoy, Japan). IR spectra were experimented on a Nicolet 5700 spectrophotometer *via* FT-IR microscope (Thermo Electron Scientific Instruments Corp.). NMR spectra was recorded on a Bruker AVIIIHD 600 (Bruker Corp., Karlsruhe, Germany) in DMSO-d_6 at 600 MHz for ^{1}H NMR and 150 MHz for ^{13}C NMR, respectively, with solvent peaks used as references. HR-ESI-MS was measured on an Agilent 1100 series (Agilent Technologies, Ltd., Santa Clara, CA, USA). Sephadex LH-20 (Pharmacia Biotech AB, Uppsala, Sweden) was used for the open column chromatography. The medium pressure liquid chromatography was performed on Combi Flash Rf 2151320193 (Teledyne Isco, Lincoln NE, USA) and equipped with a dual pump gradient system, a UV preparative detector monitoring at 254 and 210 nm, a fraction collector system and a RP-C18 column (Sepaflash, sw080, 20–45 μmol/L, Santai Technologies, Jiangsu, China). The semi-preparative HPLC was performed on SSI series 1500 (CoMetro Technology Ltd., NJ, USA) equipped with a DAD detector and a phenyl-hexyl column (250 mm × 10 mm, 5 μm, Phenomenex luna, CA, USA).

2.7. Fermentation, extraction and purification of secondary metabolites

The large-scale fermentation material of mutant *Ng*-OE was cultivated on MEPA medium at 28 °C for 7 days (280 plates, 140 mm) before collected into a 10 L vessel, and ultrasonic extracted with 7 L EtOAc (each 2 h × 4 times). The organic layer was evaporated to give a crude residue (*ca*. 37.79 g), which was then dissolved with ACN and subsequently partitioned by petroleum ether to yield a PE layer (*ca*. 33.12 g) and an ACN layer (*ca*. 4.64 g). The ACN layer was subjected to MCI column chromatograph, eluted with ACN–H_2O (20:80, 50:50 and 100:0, *v*/*v*), and acetone, to give four fractions (Fr. 1–Fr. 4). Fr. 2 (2.9747 g) was applied to a RP-18 CC (eluted with an ACN–H_2O, 25% for 5 min, 25%–60% for 35 min, 60% for 15 min and 70% for 20 min) to yield ten subfractions (Fr. 2.1–Fr. 2.10). Fr. 2.8 (346.3 mg) was then chromatographed on sephadex LH-20, eluted with MeOH giving eight subfractions (Fr. 2.8.1–Fr. 2.8.8). Fr. 2.8.4 (226.7 mg) was subjected to a semi-preparative HPLC to yield compounds **2** (0.9 mg, t_R = 36.86 min) and **3** (74.3 mg, t_R = 18.15 min). Fr. 3 (1.0215 g) was subjected to a RP-18 CC (eluted with an ACN–H_2O, 45% for 7 min, 45%–85% for 20 min, 85% for 25 min and 100% for 20 min) to yield seven subfractions (Fr. 3.1–Fr. 3.7). Fr. 3.4 (154.2 mg) was then chromatographed on a semi-preparative HPLC to yield compounds **1** (4.4 mg, t_R = 108.16 min) and **4** (1.6 mg, t_R = 132.17 min).

2.7.1. Berkeleyacetal D (*1*)

Light yellow amorphous powder; $[\alpha]_D^{25}$ 31 (*c* 1.66, MeCN; UV (MeCN) λ_{max} (logε) nm 208 (3.99), 267 (3.84). IR ν_{max} 3065, 2983, 2908, 1767, 1707, 1604, 1671, 1397, 1318, 1297, 1262, 1222, 1155, 1116, 981, 932, 871, 768, 709 cm^{-1}; For ^{1}H and ^{13}C NMR

Table 1 Genes required for berkeleyacetals biosynthesis in *Neosartorya glabra*.

Gene	aa No.	Proposed function	Coverage/identity	Protein homologue, organism	Accession No.
berA	747	C6 transcription factor protein	90/33	Transcription factor, *T. benhamiae*	XP_003012811
berB	377	thioredoxin-like protein AAED1	53/67	Thioredoxin, *P. subrubescens* 132785	OKO98901
berC	431	cytochrome P450 monooxygenase	99/83	PrhB, *P. brasilianum* NBRC 6234	BAV69303
berD	174	NAD-dependent epimerase	100/67	PrhC, *P. brasilianum* NBRC 6234	BAV69304
berE	579	MFS general substrate transporter	89/47	PrhG, *L. palustris* CBS 459.81	OCK75213
berF	170	NAD-dependent epimerase	90/31	PrhC, *P. brasilianum* NBRC 6234	BAV69304
berG	239	Terpene cyclase	94/49	PrhH, *P. brasilianum* NBRC 6234	BAV69309
berH	170	O-acetyltransferase	85/34	AusQ, *A. calidoustus*	CEL11256
berI	645	Flavin-containing monooxygenase-like	91/54	PrhJ, *P. brasilianum* NBRC 6234	BAV693011
berJ	358	FAD-dependent hydroxylase	69/60	PrhF, *P. brasilianum* NBRC 6234	BAV69307
berK	257	Short-chain dehydrogenase/reductase	100/63	PrhI, *P. brasilianum* NBRC 6234	BAV693010
berL	279	methyltransferase	100/64	PrhM, *P. brasilianum* NBRC 6234	BAV693014
berM	643	Flavin-containing monooxygenase-like	97/67	PrhK, *P. brasilianum* NBRC 6234	BAV693012
berN	512	cytochrome P450 monooxygenase	91/44	AusG, *A. flavus* NRRL3357	XP_002384778
berO	309	UbiA prenyltransferase	93/53	PrhE, *P. brasilianum* NBRC 6234	BAV693006
berP	2458	NR-PKS	99/51	PrhL, *P. brasilianum* NBRC 6234	BAV693013
berQ	133	RutC family protein(isomerase)	78/70	RutC family protein, *P. fici* W106-1	XP_007841478
berR	290	phytanoyl-CoA dioxygenase	98/74	PrhA, *P. brasilianum* NBRC 6234	BAV69302
berS	434	Cytochrome P450, putative	94/66	PrhD, *P. brasilianum* NBRC 6234	BAV69305
berT	446	Cytochrome P450, putative	100/64	AusG, *A. nidulans* FGSC A4	XP_682517

Note: *T*, *Trichophyton; L, Lepidopterella; P*, *Penillium* or *Pestalotiopsis*; *A*, *Aspergillus*.

spectroscopic data, see Table 1; HR-ESI-MS (positive-ion mode) *m/z* 449.1567 $[M + Na]^+$ (Calcd. for $C_{24}H_{26}O_7Na$, 449.1571).

2.7.2. *11-epi-Berkeleyacetal C (**2**)*

Light yellow amorphous powder; $[\alpha]_D^{25}$ –28.8 (*c* 0.66, MeCN; UV (MeCN) λ_{max} (logε) nm 200 (3.49), 227 (3.52), 270 (3.79). IR ν_{max} 3082, 2983, 2938, 1786, 1736, 1710, 1659, 1455, 1392, 1372, 1294, 1198, 1128, 1080, 1008, 931, 872, 845, 591, 539 cm^{-1}; For ^1H and ^{13}C NMR spectroscopic data, see Table 1; HR-ESI-MS (positive-ion mode) *m/z* 465.1503 $[M + Na]^+$ (Calcd. for $C_{24}H_{28}O_8Na$, 465.1520).

2.8. *X-ray crystal structure analysis*

Colorless crystals of **1** were obtained in MeOH. Intensity data was collected at Rigaku MicroMax 002+ X-ray diffractometer equipped with a CCD, using CuKα radiation. The structures were solved by direct methods using SHELXS-97. Refinements were performed with SHELXL-97 using full-matrix least-squares, with anisotropic displacement parameters used for all the non-hydrogen atoms. The H atoms were placed in the calculated positions and refined using a riding model. Molecular graphics were computed with PLATON. Crystallographic data (excluding structure factor tables) for the structure reported has been deposited with the Cambridge Crystallographic Data Center as supplementary publication No. CCDC 1567469 for **1**. Copies of the data can be obtained free of charge on application to CCDC, 12 Union Road, Cambridge CB 1EZ, UK [fax: Int. + 44 (0) (1223) 336 033; email: deposi@ccdc.cam.ac.uk].

2.9. *Crystallographic data for berkeleyacetal D (**1**)*

$C_{24}H_{26}O_7$, MW = 426.45, orthorhombic system, space group $P2_12_12_1$, cell parameter $Z = 4$, $a = 10.908$ (5) Å, $b = 12.474$ (7) Å, $c = 15.344$ (7) Å; $\alpha = \beta = \gamma = 90°$, $V = 2078.8$ (18) $Å^3$, $T = 295$ K, μ (Cu Kα) = 0.824 mm^{-1}, 649 reflections measured, 3863 independent reflections. The final R_1 value was 0.0381. The final wR_2 (F^2) value was 0.0977 [$I \geq 2\sigma(I)$], $S = 1.040$. Flack parameter = 0.07 (8).

3. Results and discussion

3.1. *Genome mining of paraherquonin-like gene cluster in N. glabra and bioinformatic analysis*

The Illumina HiSeq. 2500 `sequencing of *N. glabra* CGMCC 32286 generated a total of ~1152 million bases with an average sequencing read length of 125 bases. Assembly of the unpaired shotgun sequence reads resulted in 66 contigs, which consists of 35.16 million nonredundant bases. The draft genome of *N. glabra* was then annotated using SOAP denovo program[23]. Bioinformatic analysis using antiSMASH[24] revealed the organism could encode 12 biosynthetic gene clusters that may contain a NR-PKS, in which one biosynthetic gene cluster on contig 11 exhibited 20% similarity to terretonin. For our genomics-driven discovery of natural products and their biosynthetic mechanisms, we focused on the gene cluster designated as *ber* that resembles to paraherquonin biosynthetic cluster *prh* in *P. brasilianum* NBRC 6234. DNA sequence analysis of a contiguous ~58 kb *ber* locus (Table 1) revealed the presence of 20 putative open reading frames (*berA*–T) that might be responsible for meroterpenoid biosynthesis. *berP* putatively encodes an iterative nonreducing PKS and has a domain architecture of SAT-KS-MAT-PT-ACP-CM-TE as ascertained by *in silico* analysis. Amino acid sequence alignment indicated that BerP shares 55% identity to AdrD, a known fungal iterative PKS from *Penicillium roqueforti* involved in Andrastin A biosynthesis[28], followed by MpaC[29], PrhL[8], AusA[30,31], and Trt4[32], members of fungal DMOA-derived meroterpenoid PKSs.

Investigation of the flanking regions of the PKS gene allowed the discovery of other genes coding typical enzymes for meroterpenoid biosynthesis (Table 1). Other than genes with corresponding or homologous open reading frames in *prh* gene cluster for paraherquonin biosynthesis in *P. brasilianum* NBRC 6234, additional genes including

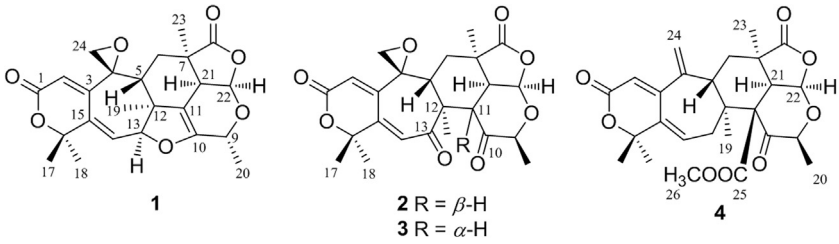

Figure 1 Structures of compounds **1**–**4**.

Table 2 ^{1}H NMR (600 MHz) and ^{13}C NMR (150 MHz) spectral data of compounds **1**–**2**[a] (δ in ppm, J in Hz, DMSO-d_6).

No.	**1**		**2**	
	δ_H	δ_C	δ_H	δ_C
1		162.5		161.7
2	5.79, d (1.2)	114.8	6.10, d (1.6)	117.6
3		155.0		150.0
4		57.7		59.1
5	2.33, dd (12.3, 4.2)	37.2	1.51, dd (14.3, 3.4)	44.3
6a	1.62, (overlap)	26.7	2.15, dd (14.3, 3.4)	28.3
6b	1.54, dd (14.6, 12.3)		1.66, t (14.3)	
6b	1.54, dd (14.6, 12.3)		1.66, t (14.3)	
7		46.1		44.9
8		177.3		176.1
9	4.34, qd (6.7, 2.4)	62.6	4.49, q (7.4)	76.3
10		149.0		207.2
11		105.5	3.12, d (14.0)	48.1
12		47.1		47.3
13	5.13, d (2.5)	89.9		201.7
14	6.18, dd (2.5, 1.2)	128.2	6.43, d (1.6)	127.1
15		132.5		145.7
16		82.7		83.2
17	1.44, s	25.5	1.43, s	28.2
18	1.60, s	25.2	1.69, s	26.2
19	1.25, s	19.1	1.17, s	12.5
20	1.28, d (6.7)	17.6	1.34, d (7.4)	17.7
21	3.02, dd (4.4, 2.4)	40.0	2.86, dd (14.0, 4.5)	41.1
22	6.24, d (4.4)	97.2	6.29, d (4.5)	97.9
23	1.26, s	23.2	1.31, s	23.5
24a	3.18, d (5.4)	55.1	2.89, d (5.4)	56.8
24b	2.64, d (5.4)		2.57, d (5.4)	
24b	2.64, d (5.4)		2.57, d (5.4)	

[a]The assignments were based on DEPT, ^{1}H–^{1}H COSY, HSQC, HMBC experiments.

berB, *berH*, *berQ*, and *berT*, exist in *ber* gene cluster. Sequence alignments and phylogenetic analysis to other meroterpenoid biosynthetic pathways, we speculated that *ber* biosynthetic cluster would be responsible for production of novel DMOA-derived meroterpenoids.

3.2. *gpdA Promoter-controlled overexpression of berA induce metabolite production*

Detailed analyses of the gene *berA* revealed the deduced BerA was related to the C6 transcriptional factor of *Trichophyton equinum* CBS 127.97 (EGE06077). To prove the concept that constitutive overexpression of a regulatory gene can lead to activation or up-regulation of the *ber* gene cluster, we amplified the putative activator gene *berA* from genomic DNA and *gPdA* promoter from plasmid pRF-HUE[33] and cloned them into G418 resistant vector pYWL42. Transformation of *N. glabra* with the plasmid harboring *berA* under the control of the constitutive glyceraldehyde-3-phosphate dehydrogenase promoter *gPdA* of *A. nidulans* resulted in several mutant strains that harboring the expression cassette, and we named one desired mutant strain, *Ng*-OE: *berA*. RT-PCR analysis showed that transcription level of *ber* biosynthetic cluster in mutant *Ng*-OE: *berA* is much higher than that in wild type strain (Supplementary Information Fig. S1), in which four genes including *berM*, *berP*, *berR*, and *berT* were selected for detection. As a result, we sought to monitor the production of new metabolites in the mutant. Notably, UPLC coupled diode array and mass detectors revealed that the induced strain produces more compounds than wild type strain (Supplementary information Fig. S2). To get sufficient amounts of compounds for full structure elucidation, a large-scale of cultivation of the overexpressing mutant strain of *N. glabra* was carried out, which led to the isolation of two new compounds berkeleyacetal D (**1**) and 11-*epi*-berkeleyacetal C (**2**), along with two known ones, berkeleyacetal C (**3**)[3] and purpurogenolide C (**4**)[34] (Fig. 1). Berkeleyacetal D (**1**) was obtained as colorless crystals with its molecular formula of $C_{24}H_{26}O_7$ confirmed by HR-ESI-MS ($[M+Na]^+$ m/z 449.1567, Calcd. 449.1571), indicating an unsaturation of 12 degrees. Its IR spectrum gave absorption bands at 3065, 1666, 1604, 841 cm^{-1}, and 1767, 1707 cm^{-1}, suggesting the presence of olefinic groups and two types of carbonyl groups, respectively. The ^{1}H NMR data (Table 2) displayed characteristic resonances for five methyls at δ_H 1.25, 1.26, 1.44, 1.60 (each 3H, s) and 1.28 (3H, d, J = 6.7 Hz). The ^{13}C NMR and DEPT spectroscopic data (Table 2) exhibited 24 carbon signals, including five methyls, corresponding to the ^{1}H NMR data, two methylenes (one oxygenated), seven methines (three oxygenated and two olefinic) and ten quaternary carbons (two ester carbonyl). Preliminary inspection of NMR spectra of **1** suggested that it was a high oxygenated and condensed compound with structure similar to paraherquonin[8] except that one oxygenated quaternary carbon (δ_C 73.3) and one methyl of paraherquonin was replaced by a methine (δ_C 40.0) and an epoxy group in **1**.

Detailed analyses of its 2D NMR spectra confirmed our assumption and helped furnish the planar structure of compound **1**. The HMBC correlations (Fig. 2) from H-2 (δ_H 5.79) to C-1 (δ_C 162.5), C-3 (δ_C 155.0), and C-15 (δ_C 132.5), from H_3-18 (δ_H 1.60) to C-1, C-15, C-16 (δ_C 82.7), C-17 (δ_C 25.5) suggested the presence of a δ-lactone. ^{1}H–^{1}H COSY spectrum (Fig. 2) showed two spin correlations of H-13/H-14, along with the HMBC correlations from H-14 (δ_H 6.18) to C-3 (δ_C 155.0), C-12 (δ_C 47.1), C-13 (δ_C 89.9), C-15, and C-16, from H-13 (δ_H 5.13) to C-2, C-3, C-4 (δ_C 57.7, s), C-5 (δ_C 37.2), C-12, C-14, C-15, and C-19 (δ_C 19.1), from H-5 (δ_H 2.33) to C-4, C-12, C-13, from H_2-24 (δ_H 3.18 and 2.64) to C-3, C-4, and C-5 revealed the presence

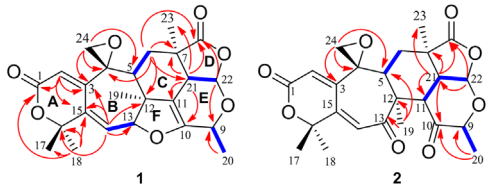

Figure 2 ^{1}H–^{1}H COSY correlations (blue bond) and selected HMBC correlations (red arrows) of **1** and **2**.

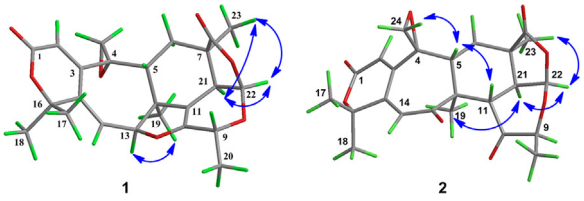

Figure 3 Selected ROESY correlations (arrows) of **1** and **2**.

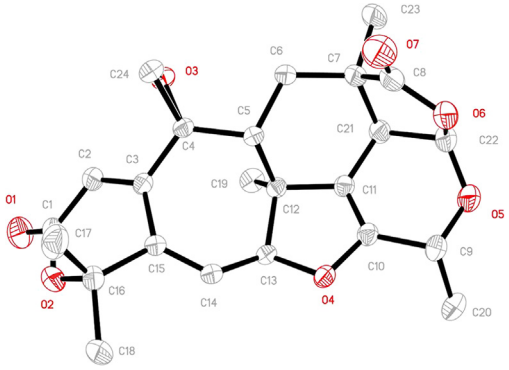

Figure 4 X-ray crystal structure of **1**.

of an unsaturated cycloheptanone and a three-membered epoxy between C-4 and C-24.

The ^{1}H–^{1}H COSY correlations of H-5/H_2-6, along with the HMBC correlations from H-5 to C-4, C-11(δ_C 105.5), C-12, and C-19, from H_2-6 (δ_H 2.15 and 1.66) to C-4, C-7 (δ_C 46.1), C-8 (δ_C 177.3), C-12, and C-21 (δ_C 40.0), constructed the ring C. ^{1}H–^{1}H COSY correlations of H-9/H_3-20, and H-21/H-22, along with HMBC correlations from H-21 (δ_H 3.02) to C-7, C-8, C-10 (δ_C 149.0), C-11, and C-23 (δ_C 23.2), from H-22 (δ_H 6.24) to C-8, C-9 (δ_C 76.3, d), C-10, C-11, C-12 and C-21, revealed a γ-lactone jointed with an unsaturated pyrane ring by C-21 and C-22, in which the dioxgenated C-22 was jointed with C-8 and C-9. The HMBC correlations from H_3-23 (δ_H 1.31) to C-6 (δ_C 28.3), C-7, C-8, and C-21, and from H_3-20 (δ_H 1.34) to C-9, and C-10 suggested the methyl groups substituted at C-7 and C-9, respectively. Given that the unsaturation degrees, the oxygenated methine C-13 (δ_C 89.9), and the HMBC correlations from H-9, H-21, and H-22 to C-10 and C-11 disclosed that F ring was a Δ^{10} unsaturated furan ring.

The relative configuration of **1** was determined by the ROESY spectrum. ROESY correlations (Fig. 3) of H-13/H_3-19, H-22/H-21/H_3-23, along with the specific optical rotation compared with berkeleyacetal C, disclosed the α-orientations of H-13, H_3-19, H-21, H-22, and H_3-23. However, the ROESY correlations of H_2-24 to H-5, and H_3-20 to H-22 could not be observed, which made it difficult to determine the relative configurations of 4,24-epoxy group and Me-20 substituent.

With the aim to confirm the absolute configuration of compound **1**, we have attempted to obtain its crystals. Fortunately, we succeeded in getting crystals of **1** from MeOH and performed the single-crystal X-ray diffraction experiment (Fig. 4). The final refinement on CuKα data resulted in a Flack parameter of 0.07 (8) allowed unequivocal assignments of the absolute configuration of the chiral carbons to be 4*R*, 5*R*, 7*R*, 21*S*, 22*R*, 9*R*, 13*S*. As a result, the configuration of 4,24-epoxy was confirmed as β-orientation, which was different to most reported berkeleyacetal-like meroterpenoids, while the Me-20 was determined to be α-orientated, which might be contributed to the formation of the F ring.

11-*epi*-Berkeleyacetal C (**2**) was obtained as light yellow amorphous powder that gave a molecular formula of $C_{24}H_{26}O_8$, as deduced by HR-ESI-MS. The IR spectra disclosed the existence of trisubstituted olefinic groups (3082, 1659, and 845 cm^{-1}), and at least three carbonyl groups (1786, 1736, and 1710 cm^{-1}). The ^{1}H NMR data (Table 2) revealed five methyls at δ_H 1.17, 1.31, 1.43, 1.69 (each 3H, s), and δ_H 1.34 (3H, d, J = 7.4 Hz), and two conjungated olefinic protons δ_H 6.43, and 6.10 (each 1H, d, J = 1.6 Hz). The ^{13}C NMR and DEPT spectra featured 24 carbons including five methyls, two methylenes, seven methines (two oxygenated and two olefinic ones), and ten carbons (two carbonyl carbons, two ester ones and two oxygenated ones). The NMR data showed that it composed a similar structure of berkeleyacetal C (**3**)[3], except for the sharp chemical shifts of C-5 ($\Delta\delta$ 12.1 ppm), C-10 ($\Delta\delta$ 4.4 ppm), C-21 ($\Delta\delta$ 4.7 ppm). The ^{1}H–^{1}H COSY correlations of H-5/H_2-6, H-11/H-21/H-22, and H-9/H_3-20, along with the HMBC correlations from H_2-24 (δ_H 2.89 and 2.57) to C-3 (δ_C 150.0), C-4 (δ_C 59.1), and C-5 (δ_C 44.3), from H_3-19 (δ_H 1.17) to C-5, C-12 (δ_C 47.3), and C-13 (δ_C 201.7), from H-21 (δ_H 2.86) to C-7 (δ_C 44.9, s), C-8 (δ_C 17.1), C-10 (δ_C 207.2), C-11 (δ_C 48.1), and C-23 (δ_C 23.5), from H-22 (δ_H 6.29) to C-8, C-11, and C-21 (δ_C 41.1), and from H_3-20 (δ_H 1.34) to C-9 (δ_C 76.3), and C-10, determined that compound **2** composing the same planar structure of **3**. Considering the chemical shifts of several positions, we deduced that the configuration of compound **2** differed from that of **3**, which was verified by the ROESY correlations. The ROESY correlations (Fig. 3) of H-24a/H-5/H_3-20/H-11, H-19/H-21/H-22/H-23, and the coupling constant of $^{3}J_{21/11}$ = 14.0 Hz and $^{3}J_{21/22}$ = 4.5 Hz revealed the *trans*-orientations of H-21 and H-11, and the *cis*-orientations of H-21 and H-22, indicating that H-11 was β-orientated. Therefore, compound **2** was an H-11 epimer of berkeleyacetal C.

Compounds **3** and **4** were identified by the comparisons of their spectroscopic data with those reported in the literatures.

3.3. *Comparative analysis of gene cluster ber with paraherquonin biosynthetic cluster prh in P. brasilianum NBRC 6234*

A more detailed bioinformatic analysis of the biosynthetic locus *ber* revealed adjacent genes that are highly homologous to previously reported *prh* cluster in *P. brasilianum* genome[8]. Both the *ber* and *prh* clusters contain a predicted DMOA-biosynthesis encoding gene as well as other putative ORFs highly conserved across previously reported biosynthetic pathway for fungal meroterpenoids. Although the *ber* and *prh* biosynthetic clusters are rearranged and nonsyntenic, the majority of their shared gene products are >40% sequence identical, and the correspondence between each *ber* gene from *N. glabra* and the respective ORF from the *prh* biosynthetic locus of strain *P. brasilianum* NBRC

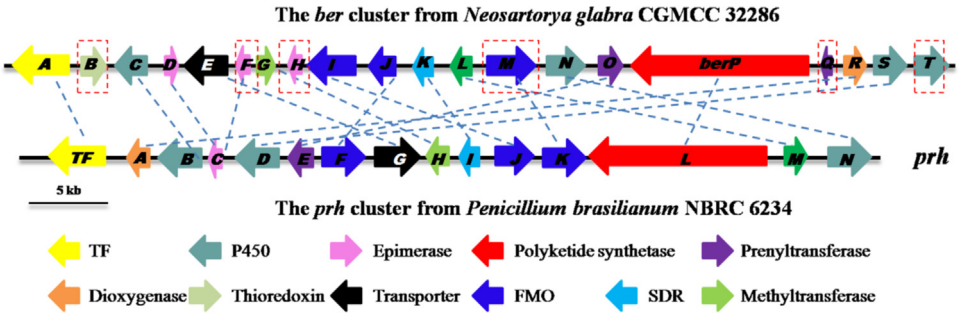

Figure 5 Schematic representation of the *ber* cluster and its nucleotide sequence comparison with the *prh* cluster from *Penicillium brasilianum* NBRC 6234.

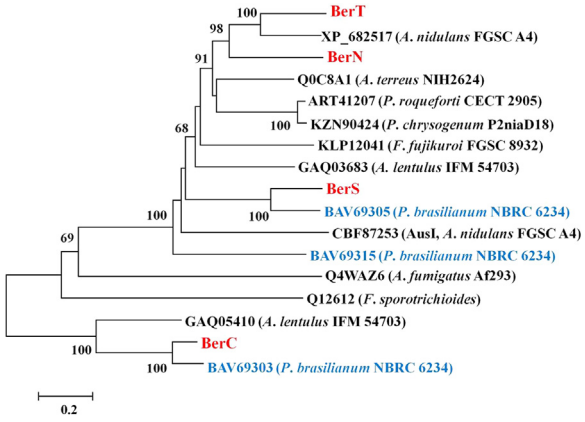

Figure 6 The full-length amino acid sequences of BerC, BerN, BerS, and BerT with other P450 oxygenases were used to construct a phylogenetic tree by the neighbor-joining method[40]. The bootstrap scores are based on 1000 reiterations. The BerC and PrhB in paraherquonin biosynthetic pathway are used as an outgroup. P450 oxygenases in berkeleyacetals and paraherquonin pathways are shown in red and blue color, respectively.

6234 is described (Table 1, Fig. 5). As shown in Fig. 5, compared to *prh* cluster, the *ber* locus is a larger biosynthetic cluster. Among them, BerB shares 67% and 39% amino acid identity to thioredoxin-like protein and AhpC antioxidant enzyme of *Penicillium subrubescens* CBS 132785 and *Pochonia chlamydosporia* 170, respectively. Also, BerB shares 27% amino acid identity to Pyr7 AndG, which are responsible for the biosynthesis of meroterpenoids including pyripyropene A[35] and anditomin[36]. Amino acid sequence alignment indicated that BerT is homologous to AusG from *Aspergillus nidulans* FGSC A4 (XP_682517, 64% identity) and followed by the Trt6 from *Penicillium roqueforti* CECT 2905 (ART41207, 47% identity)[30,32]. BerQ belongs to RutC family protein including reductases, deminases, or isomerases, whose real function needs to be further characterized.

Interestingly, there are four P450 monooxygenase coding genes in *ber* cluster including *berC*, *berN*, *berS*, and *berT*. To clarify the phylogenetic relationship of them with other P450 monooxygenases, a neighbor-joining tree was constructed using the amino acid sequence[37], as shown in Fig. 6. In this tree, BerN, BerS, and BerT formed a distinct group with AusG of *A. nidulans* FGSC A4 (XP_682517)[30], which is located to the branch of Trt6 in *A. terreus* NIH2624 (Q0C8A1)[38], FmaG in *A. fumigatus* Af293 (Q4WAZ6)[39], Tri4 in *F. sporotrichioides* (Q12612)[40], PrhD and PrhN in *P. brasilianum* NBRC 6234[8]. Moreover, BerC and PrhB constitutes into a different branch. These results suggest that mechanism of BerC is different from the other three P450 monooxygenases including BerN, BerS, and BerT.

3.4. *Proposed biosynthetic pathway of the ber cluster for meroterpenoid berkeleyacetals*

Since the biosynthetic pathway up to preaustinoid A1 has already been elucidated in meroterpenoids including austinol[29,30], austinoid[41], and paraherquonin,[1,2,8] a putative biosynthetic pathway of berkeleyacetals was envisioned (Fig. 7) based on their chemistry structures and deduced gene functions of the new gene cluster data. The domain organization of the NR-PKS encoded by *berP* is similar to other reported PKS genes, including AndM in *A. stellatus* (54% identity to BerP), AusA in *A. nidulans* (53% identity to BerP), Trt4 in *A. terreus* (52% identity to BerP)[30,36,38]. Also the heteroexpression of *berP* was performed to confirm that identified pathway in *N. glabra* was correctly annotated, in which 3, 5-dimethylorsellinic acid was isolated and characterized (Supplementary information Fig. 1). Moreover, due to the gene products of *ber* cluster including BerO, BerL, BerJ, BerG, BerK, BerI, BerM, and BerR share high similarity (42%–64%) to those proteins characterized in *and*, *aus*, and *prh* biosynthetic clusters, which were shown to produce meroterpenoids including andito Fig, austinol and paraherquonin[1,8,30,36]. We reasoned that preaustinoid A1 (**13**) and berkeleydione (**15**) should be the common intermediates on-pathway in berkeleyacetals biosynthesis. We hypothesized that DMOA (**5**) is directly farnesylated by BerO, followed by sequential reactions including the methyl ester-forming by BerL, (*S*)-expoxidation and 3α-hydroxylation by BerJ, respectively. The cyclization and formation of tetracyclic protoaustinoid A (**10**) from epoxyfarnesyl-DMOA methylester (**9**) could be mediated by BerG, which has protein sequence similarity to discovered terpene cyclases (PrhH, 49% identity and AusL, 42% identity)[8,30]. The hypothetic formation of preaustinoid A (**12**) by BerK and BerI is supported by the high sequence similarity to short-chain dehydrogenase and flavin-containing monooxygenase (57% protein similarity with *and* homologues, AndC and AndE)[36]. Based on the Baeyer-Villiger oxidation functions of its homologues, we proposed that BerM undergoes Baeyer-Villiger oxygen insertion to generate ϵ-lactone ring system in preaustinoid A1 (**13**). BLAST analysis showed that BerR has 76% and 74% amino acid identity to AusE and PrhA, which belong to multifunctional Fe (II)/α-ketoglutate (α-KG)-dependent dioxygenases family[8,31], we deduce that BerR encodes a dioxygenase that catalyzes the construction of cycloheptadiene moiety into berkeleydione (**15**) from preaustinoid A1 (**13**) *via* the same mechanism

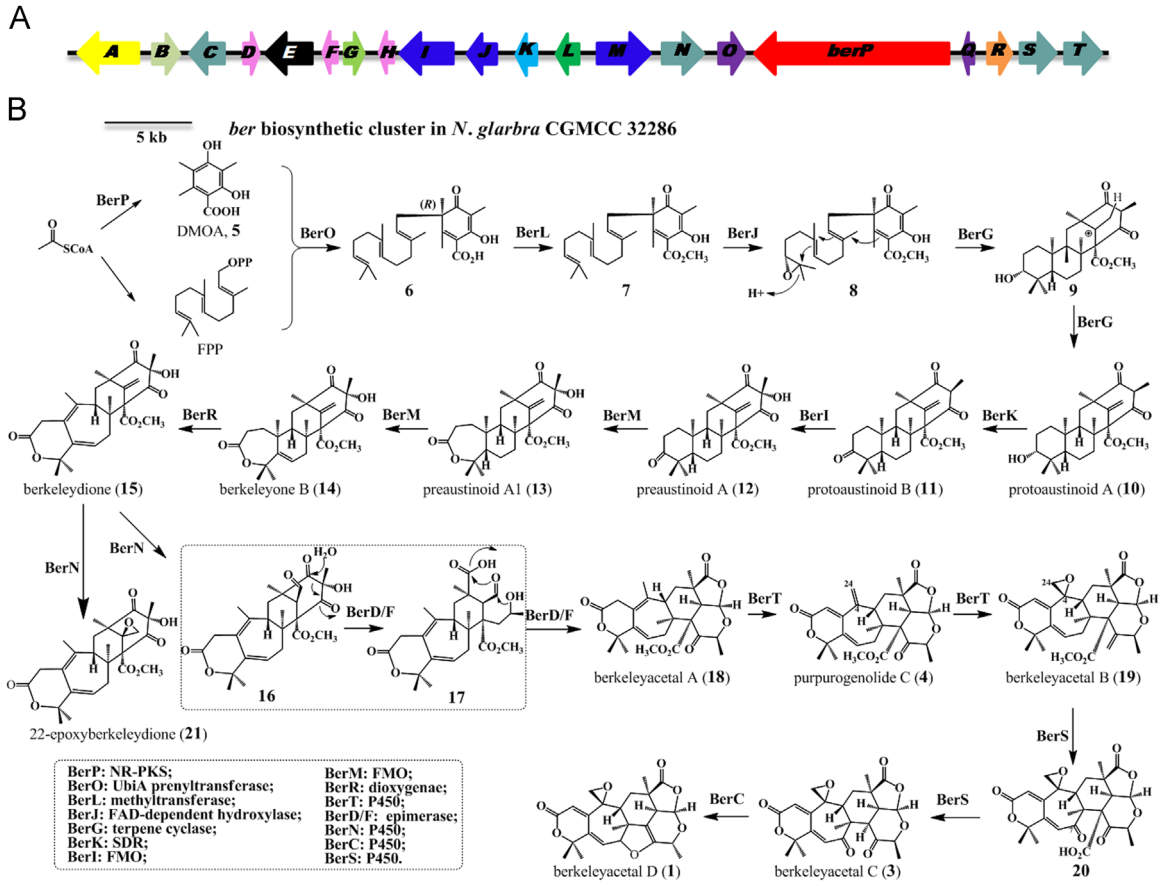

Figure 7 Proposed biosynthetic pathway of berkeleyacetals. (A) *ber* biosynthetic cluster in *N. glarbra* CGMCC 32286; (B) Hypothetical biosynthetic pathway of berkeleyacetals.

during paraherquonin biosynthesis[8]. The multifunctional dioxygenase BerR is the central player in the consecutive oxidations and structural rearrangement from "7+6" bicycle skeleton in **13** to "6+7" bicycle skeleton in **15**.

Upon formation of the on-pathway tetracyclic intermediate berkeledione (**15**), multistep oxidation at distinct carbon atoms of substrates are required to afford the final berkeleyacetal D (**1**) and 11-*epi*-berkeleyacetal C (**2**). Previous studies demonstrated that cyclopropane formation of natural products could be catalyzed by cytochrome P450 oxygenases, examples including fumagillin[42], cytochalasins[43], aureothin[44]. Similarly, we propose that the oxidative modifications at *exo*-methylene position of berkeledione (**15**), and C4–C24 epoxidation of berkeleyacetal B (**19**) are likely to be catalyzed by the two cytochrome P450 oxygenases, BerN and BerT. As shown in Fig. 1, chemical structure of berkeleyacetal D and paraherquonin are similar except the generation of C4–C24 epoxide in former compound, indicates the parallel hidden biosynthetic mechanisms. This implies that BerT is most likely dedicated to the reaction for there is no homologue of BerT in *prh* gene cluster[8]. The berkeleyacetals were previously isolated from fungal strains *P. rubrum* Berkeley Pit[3], *P. purpurogenum* MHZ111[34], and a marine mangrove-derived *Penicillium* sp. MA-37 which should be *P. verruculosum* MA-37 with 99% ITS identity)[45]. However, it has not been reported from strain *P. brasilianum* to the best of our knowledge.

BerN and BerS exhibits 47% and 25% protein identity to BerT, respectively, and this implies BerN possibly could be responsible for the oxidization from *exo*-methylene on C-22 to an aldehyde in compound **16** (Fig. 7), the epoxide-containing off-pathway compound 22-epoxyberkeleydione (**21**) could be the shunt product generated simultaneously[1]. The existence of **21** is supported by the isolation and characterization of 22-epoxyberkeleydione in strain *Penicillium* sp. MA-37 and *P. minioluteum*[45,46]. The BerS is proposed to involve the C-7 oxidation and elimination of the methyl ester group followed by the spontaneous decarboxylation of the β-keto acid, which shares 34% amino acid identity to the well-known multifunctional P450 oxygenase Trt6. This coincides with the proposed role of Trt6 being involved in the formation of terretonin H during terretonin biosynthesis[32,47]. The last P450 monoxygenase might be participating in ether bond formation in compound berkeleyacetal D (**1**) through dehydration. The hypothesis proposed is supported by the high sequence similarity of BerC to PrhB encoded by *prh* biosynthetic cluster (82% protein identity), and the structural similarity of the product berkeleyacetal D to paraherquonin. Also, there is no P450 oxygenase homologues in other meroterpenoids biosynthesis to the best of our knowledge[1,28,30,32,36,41,47]. As shown in Fig. 7, two epimerases including BerD or BerF could be proposed involving the rearrangement of intermediates, and the similarity of BerD or BerF to the AusH (28% amino acid identity) in the austinol pathway supports the proposed function of two proteins[30]. Therefore, the biosynthetic pathway from tetracyclic intermediate berkeledione (**15**) to highly oxygenated berkeleyacetals is proposed: BerN, a P450 monooxygense, catalyzed an oxygenation coupled to generation of aldehyde group, followed by structural rearrangement and a second epoxidation that results in the conversion of berkeleyacetal A to berkeleyacetal B.

The P450 oxygenases BerS and BerC are believed to involve the conversions of berkeleyacetal C and berkeleyacetal D, respectively. In addition, the various stereochemistry at C_9 and C_{11} in berkeleyacetals may due to the enolixatian of C_{10} carbonyl and keto-enol tautomerization.

4. Conclusions

We have identified a cryptic or down-regulated meroterpenoid gene cluster *ber* by genome mining, and successfully developed a strategy to activate the gene cluster by overexpressing pathway-specific regulator gene in *N. glabra*. As a result, we were able to isolate and characterize four berkeleyacetal derivatives (**1**–**4**). Moreover, bioinformatic analysis of the *ber* gene cluster was performed which helped to uncover a number of intriguing aspects of berkeleyacetals biosynthetic pathway. Further investigation on the multifunctional P450 oxygenases, including gene disruption (*e.g., ΔberT*, *ΔberN* and *ΔberC*), on-pathway intermediates characterization and *in vitro* biochemistry, should be performed to conclusively solve the problem.

Acknowledgments

This work was supported financially by the National Natural Science Foundation of China (No. 81522043), CAMS Initiative for Innovative Medicine (2017-I2M-4-004), and the Thousand Young Talents Program of China. Youcai Hu is the Union Scholar in PUMC. We are grateful to Prof. Wenbin Yin (Institute of Microbiology, Chinese Academy of Sciences, Beijing, China) sharing plasmid pYWL42, and the Department of Instrumental Analysis of Peking Union Medical College for the spectroscopic measurements and Dr. Ningbo Gong for solving the crystal structure of **1**.

Appendix A. Supporting information

Supplementary data associated with this article can be found in the online version at https://doi.org/10.1016/j.apsb.2017.12.005.

References

1. Matsuda Y, Abe I. Biosynthesis of fungal meroterpenoids. *Nat Prod Rep* 2016;**33**:26–53.
2. Geris R, Simpson TJ. Meroterpenoids produced by fungi. *Nat Prod Rep* 2009;**26**:1063–94.
3. Stierle DB, Stierle AA, Patacini B. The berkeleyacetals, three meroterpenes from a deep water acid mine waste *Penicillium*. *J Nat Prod* 2007;**70**:1820–3.
4. Stierle A, Stierle D, Decato D. Redetermination and absolute configuration of berkeleydione. *Acta Crystallogr E Crystallogr Commun* 2015;**71**:o248.
5. Stierle DB, Stierle AA, Hobbs JD, Stokken J, Clardy J. Berkeleydione and berkeleytrione, new bioactive metabolites from an acid mine organism. *Org Lett* 2004;**6**:1049–52.
6. Centko RM, Williams DE, Patrick BO, Akhtar Y, Garcia Chavez MA, Wang YA, et al. Dhilirolides E–N, meroterpenoids produced in culture by the fungus *Penicillium purpurogenum* collected in Sri Lanka: structure elucidation, stable isotope feeding studies, and insecticidal activity. *J Org Chem* 2014;**79**:3327–35.
7. de Silva ED, Williams DE, Jayanetti DR, Centko RM, Patrick BO, Wijesundera RL, et al. Dhilirolides A–D, meroterpenoids produced in culture by the fruit-infecting fungus *Penicillium purpurogenum* collected in Sri Lanka. *Org Lett* 2011;**13**:1174–7.
8. Matsuda Y, Iwabuchi T, Fujimoto T, Awakawa T, Nakashima Y, Mori T, et al. Discovery of key dioxygenases that diverged the paraherquonin and acetoxydehydroaustin pathways in *Penicillium brasilianum*. *J Am Chem Soc* 2016;**138**:12671–7.
9. Elissawy AM, El-Shazly M, Ebada SS, Singab AB, Proksch P. Bioactive terpenes from marine-derived fungi. *Mar Drugs* 2015;**13**:1966–72.
10. Bergmann S, Schumann J, Scherlach K, Lange C, Brakhage AA, Hertweck C. Genomics-driven discovery of PKS-NRPS hybrid metabolites from *Aspergillus nidulans*. *Nat Chem Biol* 2007;**3**:213–7.
11. Chooi Y-H, Fang J, Liu H, Filler SG, Wang P, Tang Y. Genome mining of a prenylated and immunosuppressive polyketide from pathogenic fungi. *Org Lett* 2013;**15**:780–3.
12. Gressler M, Zaehle C, Scherlach K, Hertweck C, Brock M. Multifactorial induction of an orphan PKS-NRPS gene cluster in *Aspergillus terreus*. *Chem Biol* 2011;**18**:198–209.
13. Mao XM, Xu W, Li D, Yin WB, Chooi YH, Li YQ, et al. Epigenetic genome mining of an endophytic fungus leads to the pleiotropic biosynthesis of natural products. *Angew Chem Int Ed Engl* 2015;**54**:7592–6.
14. Bai Jian, Mu Rong, Dou Man, Yan Daojiang, Liu Bingyu, Wei Qian, et al. Epigenetic modification in histone deacetylase deletion strain of *Calcarisporium* arbuscula leads to diverse diterpenoids. *Acta Pharm Sin* B 2018. Available from: 〈http://dx.doi.org/10.1016/j.apsb.2017.12.012〉.
15. Yang XL, Awakawa T, Wakimoto T, Abe I. Three acyltetronic acid derivatives: noncanonical cryptic polyketides from *Aspergillus niger* identified by genome mining. *Chembiochem* 2014;**15**:1578–83.
16. Nakazawa T, Ishiuchi K, Praseuth A, Noguchi H, Hotta K, Watanabe K. Overexpressing transcriptional regulator in *Aspergillus oryzae* activates a silent biosynthetic pathway to produce a novel polyketide. *Chembiochem* 2012;**13**:855–61.
17. Awakawa T, Yang XL, Wakimoto T, Abe I. Pyranonigrin E: a PKS-NRPS hybrid metabolite from *Aspergillus niger* identified by genome mining. *Chembiochem* 2013;**14**:2095–9.
18. Jayasuriya H, Zink D, Basilio A, Vicente F, Collado J, Bills G, et al. Discovery and antibacterial activity of glabramycin A–C from *Neosartorya glabra* by an antisense strategy. *J Antibiot* 2009;**62**:265–9.
19. Kijjoa A, Santos S, Dethoup T, Manoch L, Almeida AP, Vasconcelos MH, et al. Sartoryglabrins, analogs of ardeemins, from *Neosartorya glabra*. *Nat Prod Commun* 2011;**6**:807–12.
20. May Zin WW, Buttachon S, Dethoup T, Fernandes C, Cravo S, Pinto MM, et al. New cyclotetrapeptides and a new diketopiperzine derivative from the marine sponge-associated fungus *Neosartorya glabra* KUFA 0702. *Mar Drugs* 2016;**14**:136.
21. Liu WH, Zhao H, Li RQ, Zheng HB, Yu Q. Polyketides and meroterpenoids from *Neosartorya glabra*. *Helv Chim Acta* 2015;**98**:515–9.
22. Zhou H, Qiao K, Gao Z, Vederas JC, Tang Y. Insights into radicicol biosynthesis *via* heterologous synthesis of intermediates and analogs. *J Biol Chem* 2010;**285**:41412–21.
23. Li R, Zhu H, Ruan J, Qian W, Fang X, Shi Z, et al. *De novo* assembly of human genomes with massively parallel short read sequencing. *Genome Res* 2010;**20**:265–72.
24. Blin K, Medema MH, Kottmann R, Lee SY, Weber T. The antiSMASH database, a comprehensive database of microbial secondary metabolite biosynthetic gene clusters. *Nucleic Acids Res* 2017;**45**:D555–9.
25. Hofrichter M, Kellner H, Pecyna MJ, Ullrich R. Fungal unspecific peroxygenases: heme-thiolate proteins that combine peroxidase and cytochrome P450 properties. *Adv Exp Med Biol* 2015;**851**:341–68.
26. Andrianopoulos A, Hynes MJ. Cloning and analysis of the positively acting regulatory gene amdR from *Aspergillus nidulans*. *Mol Cell Biol* 1988;**8**:3532–41.
27. Gao X, Chooi YH, Ames BD, Wang P, Walsh CT, Tang Y. Fungal indole alkaloid biosynthesis: genetic and biochemical investigation of

the tryptoquialanine pathway in *Penicillium aethiopicum*. *J Am Chem Soc* 2011;**133**:2729–41.
28. Rojas-Aedo JF, Gil-Durán C, Del-Cid A, Valdés N, Álamos P, Vaca I, et al. The biosynthetic gene cluster for andrastin A in *Penicillium roqueforti*. *Front Microbiol* 2017;**8**:813.
29. Regueira TB, Kildegaard KR, Hansen BG, Mortensen UH, Hertweck C, Nielsen J. Molecular basis for mycophenolic acid biosynthesis in *Penicillium brevicompactum*. *Appl Environ Microbiol* 2011;**77**:3035–43.
30. Lo HC, Entwistle R, Guo CJ, Ahuja M, Szewczyk E, Hung JH, et al. Two separate gene clusters encode the biosynthetic pathway for the meroterpenoids austinol and dehydroaustinol in *Aspergillus nidulans*. *J Am Chem Soc* 2012;**134**:4709–20.
31. Matsuda Y, Awakawa T, Wakimoto T, Abe I. Spiro-ring formation is catalyzed by a multifunctional dioxygenase in austinol biosynthesis. *J Am Chem Soc* 2013;**135**:10962–5.
32. Matsuda Y, Iwabuchi T, Wakimoto T, Awakawa T, Abe I. Uncovering the unusual D-ring construction in terretonin biosynthesis by collaboration of a multifunctional cytochrome P450 and a unique isomerase. *J Am Chem Soc* 2015;**137**:3393–401.
33. Frandsen RJ, Andersson JA, Kristensen MB, Giese H. Efficient four fragment cloning for the construction of vectors for targeted gene replacement in filamentous fungi. *BMC Mol Biol* 2008;**9**:70.
34. Sun J, Zhu ZX, Song YL, Dong D, Zheng J, Liu T, et al. Nitric oxide inhibitory meroterpenoids from the fungus *Penicillium purpurogenum* MHZ 111. *J Nat Prod* 2016;**79**:1415–22.
35. Itoh T, Tokunaga K, Matsuda Y, Fujii I, Abe I, Ebizuka Y, et al. Reconstitution of a fungal meroterpenoid biosynthesis reveals the involvement of a novel family of terpene cyclases. *Nat Chem* 2010;**2**:858–64.
36. Matsuda Y, Wakimoto T, Mori T, Awakawa T, Abe I. Complete biosynthetic pathway of anditomin: nature's sophisticated synthetic route to a complex fungal meroterpenoid. *J Am Chem Soc* 2014;**136**:15326–36.
37. Tamura K, Stecher G, Peterson D, Filipski A, Kumar S. MEGA6: molecular evolutionary genetics analysis version 6.0. *Mol Biol Evol* 2013;**30**:2725–9.
38. Guo CJ, Knox BP, Chiang YM, Lo HC, Sanchez JF, Lee KH, et al. Molecular genetic characterization of a cluster in *A. terreus* for biosynthesis of the meroterpenoid terretonin. *Org Lett* 2012;**14**:5684–7.
39. Lin HC, Chooi YH, Dhingra S, Xu W, Calvo AM, Tang Y. The fumagillin biosynthetic gene cluster in *Aspergillus fumigatus* encodes a cryptic terpene cyclase involved in the formation of *β-trans*-bergamotene. *J Am Chem Soc* 2013;**135**:4616–9.
40. Hohn TM, Desjardins AE, McCormick SP. The *Tri4* gene of *Fusarium sporotrichioides* encodes a cytochrome P450 monooxygenase involved in trichothecene biosynthesis. *Mol Gen Genet* 1995;**248**:95–102.
41. Valiante V, Mattern DJ, Schuffler A, Horn F, Walther G, Scherlach K, et al. Discovery of an extended austinoid biosynthetic pathway in *Aspergillus calidoustus*. *ACS Chem Biol* 2017;**12**:1227–34.
42. Lin HC, Tsunematsu Y, Dhingra S, Xu W, Fukutomi M, Chooi YH, et al. Generation of complexity in fungal terpene biosynthesis: discovery of a multifunctional cytochrome P450 in the fumagillin pathway. *J Am Chem Soc* 2014;**136**:4426–36.
43. Qiao K, Chooi YH, Tang Y. Identification and engineering of the cytochalasin gene cluster from *Aspergillus clavatus* NRRL 1. *Metab Eng* 2011;**13**:723–32.
44. He J, Müller M, Hertweck C. Formation of the aureothin tetrahydrofuran ring by a bifunctional cytochrome p450 monooxygenase. *J Am Chem Soc* 2004;**126**:16742–3.
45. Zhang Y, Li XM, Shang Z, Li CS, Ji NY, Wang BG. Meroterpenoid and diphenyl ether derivatives from *Penicillium* sp. MA-37, a fungus isolated from marine mangrove rhizospheric soil. *J Nat Prod* 2012;**75**:1888–95.
46. Iida M, Ooi T, Kito K, Yoshida S, Kanoh K, Shizuri Y, Kusumi T. Three new polyketide-terpenoid hybrids from *Penicillium* sp. *Org Lett* 2008;**10**:845–8.
47. Matsuda Y, Awakawa T, Mori T, Abe I. Unusual chemistries in fungal meroterpenoid biosynthesis. *Curr Opin Chem Biol* 2016;**31**:1–7.